

# Pressure drop characteristics of iron filters

## Introduction/Background

The objective of this project was to develop pressure drop data as a function of flow velocity for cellular and foam iron filters. The data was obtained via water modeling, and can be used in current computer simulation software, as well as for hand calculated performance evaluations.

Many informative articles and papers exist that discuss various aspects of filter performance from the perspective of pressure drop<sup>1-10</sup>. These papers should be studied to obtain a thorough understanding of how filters affect fluid flow, and how to accurately characterize the flow phenomena.

While some filter pressure drop data is available in the above references, the data documented is generally intended to communicate and illustrate other technical concepts, such as filter permeability and the characteristics of Ergun's and Forchheimer's equations. This paper uses these concepts, and others, to develop a complete set of pressure drop information for cellular and foam iron filters.

## Method of Analysis

The experiment setup, shown in Figure 1, consists of a continuous conduit in which water is forced to flow through a test chamber. The water flow rate can be varied, and is regulated by a centrifugal pump.

The test chamber is designed to hold a Nylamid receptacle measuring 55mm x 55mm square. Nylamid is a machinable polymer. Filters must be mounted within this receptacle, thus the size of the filter that can be tested is limited to 55mm. 44 cellular filters, ranging in dimension from 37mm to 55mm, were tested. Filter thickness ranged from 9.5mm to 12.5mm, and cells per square inch (csi) ranged from 100 to 300. 18 foam filters, each measuring 50mm square and 22mm thick, were tested at 10, 20 and 30ppi (pores per linear inch).

Figure 2 shows a 43mm x 43mm 100 cell filter mounted in the Nylamid receptacle.



Figure 2: 100 csi Filter Mounted in Nylamid Receptacle.<sup>2</sup>

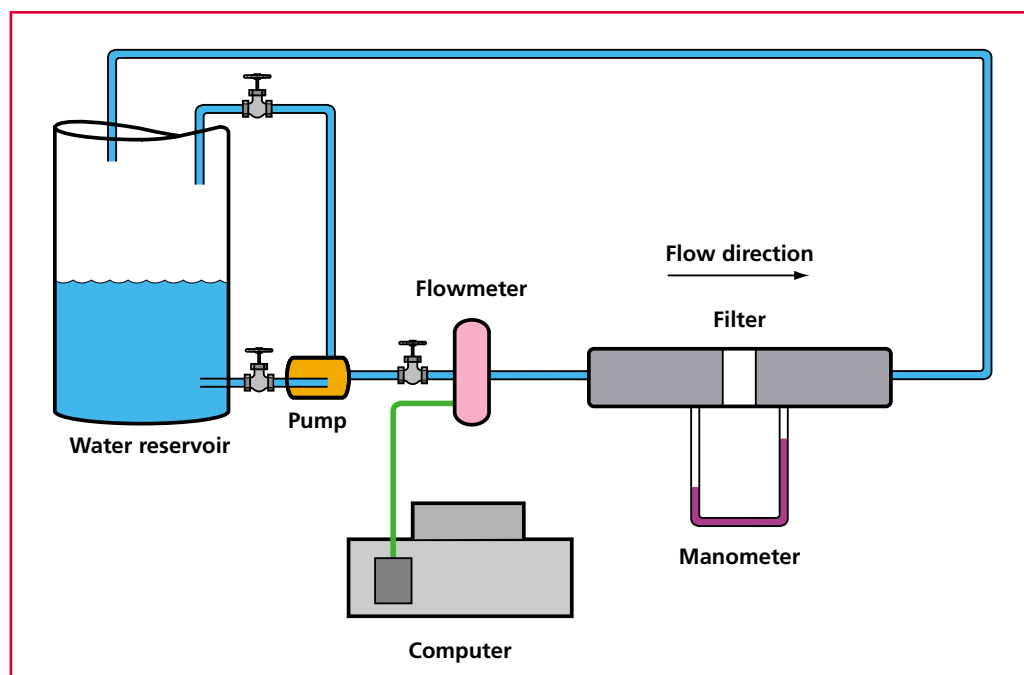


Figure 1: Schematic of Experimental Setup.<sup>2</sup>

The water flow rate is varied using 3 control valves, and is measured with an electronic flowmeter. The flow velocity test range was from 0.05 to 0.4 m/s, which represents the documented flow velocity range through a filter for iron gating systems.

Once flow velocity reaches equilibrium for a given filter, a differential manometer is used to measure the pressure drop. The differential between the manometer tubes is measured three times with a digital Vernier, and an average value of  $D_h$  is used to determine the pressure drop. Pressure drop is simply defined as:

$$D_p = \Delta p \ g \ \Delta h \quad (1)$$

$\Delta p$  is the density difference between water and the Chloroform fluid used in the manometer, and is equal to 500 kg/m<sup>3</sup>. The acceleration of gravity is defined as  $g$ , and is 9.8 m/s<sup>2</sup>.  $\Delta h$  is the differential height difference between the two manometer tubes, and is measured in meters.

For the cellular filters, two samples of each filter type were tested. One filter of each type was tested two times, once with one filter face toward the incoming flow, and a second time with the other filter face toward the incoming flow. The second filter sample was tested in only one direction. Thus, three pressure drop measurements were reported for each cellular filter type.

For the foam filters, six samples of each filter type were tested. The samples were carefully selected such that the entire range of foam variability was accounted for.

## Results and Discussion

The results from this study are enlightening. The actual pressure drop data and correlations, including the Forchheimer constants, are documented and discussed for each filter type. Also, the Darcian and non-Darcian permeability coefficients are tabulated for each filter type.

### Filter Pressure Drop Data

While the data was consistent and repeatable, a significant effort was still required to develop adequate correlations such that the data could be appropriately categorized. Accurate correlations were developed by dividing the pressure drop data by the thickness of the filter, and grouping the filters according to cell count.

Data for the foam filters also correlates strongly when pressure drop is divided by filter thickness, and is grouped by pores per inch. The R squared values range from 87% for the 10ppi filters, to over 95% for the 20 and 30ppi filters.

All of the correlations conform to the second order polynomial format of the Forchheimer's equation, given below.

$$D_p / \text{Filter Thickness} = b_1 * (\text{flow velocity}) + b_2 * (\text{flow velocity})^2 \quad (2)$$

$D_p$  is the pressure drop for water in Pascals. Flow velocity is given in m/s. The values of  $b_1$  and  $b_2$ , derived from plots of pressure drop/velocity, are given below in Table 1.

The correlations are plotted in Figure 3 where the y-axis is filter pressure drop (Pascals) divided by filter thickness (meters). The x-axis is flow velocity (m/s).

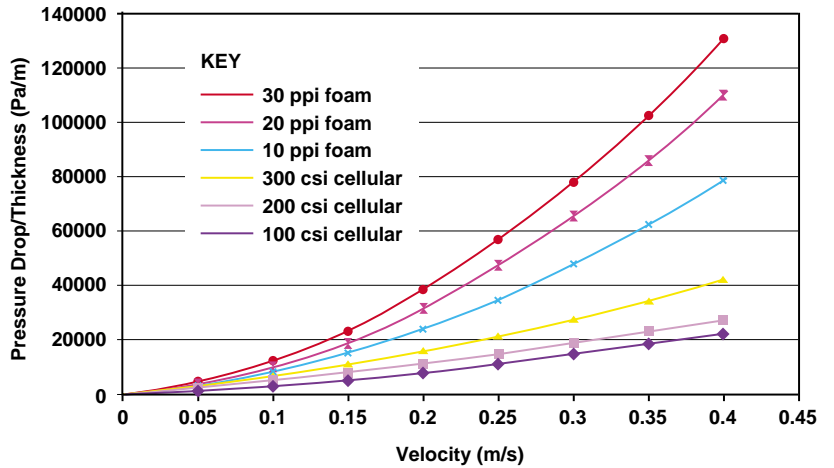


Figure 3: Cellular and Foam Filter pressure drop data correlations.

Filter Type	$b_1$ (kg/m <sup>3</sup> - s)	$b_2$ (kg/m <sup>4</sup> )	R <sup>2</sup>
Cellular 100 csi	28221	70851	0.9188
Cellular 200 csi	53477	33311	0.9933
Cellular 300 csi	58577	114434	0.9671
Foam 10ppi	46711	375408	0.8659
Foam 20ppi	38123	592484	0.9533
Foam 30ppi	55779	677299	0.9592

Table 1: Forchheimer's Coefficients for Iron Cellular and Foam Filters.

As expected, pressure drop increases with increasing cells, or pores, per inch. The 100 cells per inch cellular filter has the lowest pressure drop curve, followed by the 200 and 300 csi cellular filters, respectively. 10 ppi foam filters have a lower pressure drop curve than both the 20 and 30 ppi foam filters, respectively. However, all of the foam filters have significantly higher pressure drop characteristics than cellular filters.

### Adjusting the Data for Molten Metal

The data given in the figures and tables above represents filter pressure drop characteristics as a function of water flow velocity. A simple procedure can be applied to adjust the data to represent molten metal fluid flow.

It has been well documented in the literature that the shape of the filter pressure drop curve as a function of flow velocity is a quadratic function. In fact, the equations, as shown above, generally take on the form:

$$D_p / L = b_1 * u + b_2 * u^2 \quad (3)$$

Equations (2) and (3) are known as Forchheimer's equation.  $D_p$  is the pressure drop,  $L$  is the filter thickness,  $u$  is the flow velocity and  $b_1$  and  $b_2$  are the Forchheimer's coefficients. In fact,  $b_1$  and  $b_2$  are defined as follows:

$$b_1 = \mu / k_1 \quad (4)$$

$$b_2 = \rho / k_2 \quad (5)$$

$\mu$  is the dynamic viscosity, and  $\rho$  is the density.  $k_1$  is called the Darcian permeability, and is related to energy losses in the fluid stream caused by viscous attrition.  $k_2$  is called the non-Darcian permeability, and is related to energy losses in the fluid stream caused by inertial effects. The pressure drop through a filter is the sum of these two effects, and results in a non-linear relationship between filter pressure drop and flow velocity.

Filter Type	$k_1$ ( $10^{-8} \text{ m}^2$ )	$k_2$ ( $10^{-2} \text{ m}$ )
Cellular 100 csi	3.5435	1.4114
Cellular 200 csi	1.8700	3.0020
Cellular 300 csi	1.7072	0.8839
Foam 10ppi	2.1408	0.2664
Foam 20ppi	2.6231	0.1688
Foam 30ppi	1.7928	0.1476

Table 2: Darcian and non-Darcian Permeability Coefficients for Iron Filters.

$k_1$  and  $k_2$  are commonly used to describe the filter flow properties, and can be easily obtained from the Table 1 data as follows:

$$k_1 = \mu_{\text{water}} / b_1 \quad \mu_{\text{water}} = 0.001 \text{ Pa s (at 20C)} \quad (6)$$

$$k_2 = \rho_{\text{water}} / b_2 \quad \rho_{\text{water}} = 1000 \text{ kg/m}^3 \text{ (at 20C)} \quad (7)$$

Table 1 can be rewritten such that values of  $k_1$  and  $k_2$  can be documented for each filter type. These values are listed in Table 2.

These values agree well with other filter data correlated using both Darcian and non-Darcian coefficients.

Using Forchheimer's equation (3), the pressure drop through each filter can easily be calculated for any metal type, as long as the density and viscosity of the molten metal at the pouring temperature are known.

### Computer Simulations

Several casting simulations using MAGMASOFT<sup>11</sup> were conducted to validate the cellular filter pressure drop data. In each case, simulations had been previously conducted with a cellular filter dataset from the literature<sup>12</sup>. To validate the accuracy of the filter data, the predicted fill time is compared. The comparison is between the fill time predicted using the data from the literature, the predicted fill time using the data in this paper, and the actual fill time recorded in the foundry.

If the pouring conditions are known, MAGMASOFT will attempt to predict the casting fill time, in addition to the normal filling/solidification predictions. In each case, a constant pressure condition was input to simulate the metal stream as it enters the mould cavity. Both examples shown are produced on a DISA.

Figures 4 and 5 show a grey and a ductile iron casting, respectively, used to validate the filter data. Figure 4 is a crankcase casting filtered with a 43mm x 43mm square, 12.5mm thick, 300 csi cellular filter. Figure 5 is a differential case casting filtered with a 81mm x 81mm square, 12.5mm thick, 100 csi cellular filter.

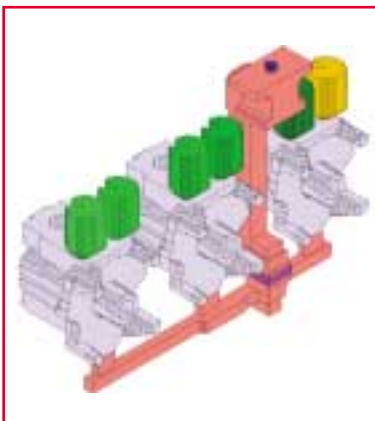


Figure 4: Gray Iron Crankcase Filtered with 43mm x 43mm x 12.5mm, 300 csi Cellular Filter.

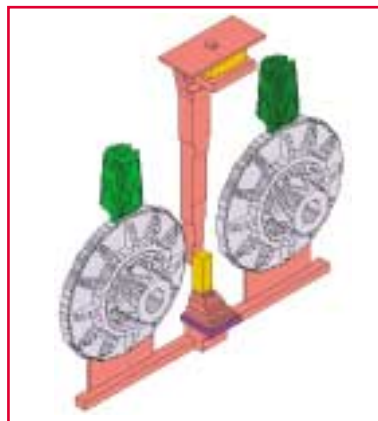


Figure 5: Ductile Iron Differential Case Casting Filtered with 81mm x 81mm x 12.5mm, 100 csi Cellular Filter.

Casting	Actual Pour Time (sec)	Predicted Pour Time w/ Prev Data (sec)	Predicted Pour Time w/ New Data (sec)
Crankcase	9	13.5	9.7
Differential Case	9	10.1	8.9

Table 3 summarizes the filling results.

The predicted pour time results are much closer to the actual pour time when using the newly developed data. It is likely that the longer the pour time, the larger the difference between the two filter datasets, and thus the greater the error when using the previous filter data. The accuracy of mould filling simulations should increase across the board with this new data, but will be especially apparent for the larger pour times.

Similar improved results were observed for several ductile iron casting simulations using the foam filter data, compared to standard data taken from the literature. Unfortunately, these results were foundry proprietary, and cannot be shared in an open forum.

### Summary/Conclusions

Pressure drop data was collected for 44 cellular and 18 foam filters using water flow.

Pressure drop correlations were developed for 100, 200 and 300 csi cellular iron filters and 10, 20 and 30 ppi foam iron filters. Pressure drop for these filters was dependent upon cells (pores) per square inch and filter thickness. Pressure drop decreases with decreases in cell count, and increases with increases in filter thickness. The combination of these characteristics plus the porosity determine the pressure drop curve for a filter.

Accurate correlations with confidence levels generally above 90% were developed when the filter pressure drop data was divided by filter thickness, and grouped by cell count. Foam filters showed slightly more variability in pressure drop than cellular filters, but only for 10ppi filters. Even still, correlations for the 10ppi filters achieved an 87% confidence level, which is quite good. Future work will review this situation more closely.

The pressure drop correlations were converted to a standardized description of filter flow characteristics, which involves computation of the Darcian and non-Darcian permeability coefficients. The power of these coefficients is that they are the standard for characterizing filter flow performance, and are not dependent upon the fluid medium used to collect the pressure drop data. More importantly, the pressure drop performance of the filter can be determined for any fluid flow using these coefficients, assuming that the fluid viscosity and density at the pouring temperature are known. These are the values used for computer simulation analyses.

Computer simulations were conducted for several casting configurations using MAGMASOFT. Each configuration was run with the "newly" developed data, and re-run with corresponding filter data available in the current literature. The program was given the metal flow stream information, and asked to predict the fill time. In all cases, the predicted fill time for the case using the newly developed data

more closely matched the "real" fill time (measured in the foundry), than the predicted fill time when using the previous set of filter data. This validates the accuracy and usefulness of the data for computer simulations.

As expected, filter pressure drop increased with increasing cells (or pores) per unit area of the filter. In addition, foam filters exhibit considerably higher pressure drop values than cellular filters.

### Acknowledgements

The author would like to thank FOSECO colleague Phil Dahlstrom for his invaluable assistance in preparing the many plots in this report, and for his assistance with data correlation and computer simulation. Also, Scott Limestoll and Brian Began of FOSECO made significant contributions, both in categorizing the filters to be tested, and in providing valuable details regarding filter production. Finally, Dr. A. Humberto Castillejos E., and Dr. F. Andres Acosta G. Of CINVESTAV, Saltillo, Mexico are to be commended for their outstanding work. CINVESTAV provided valuable technical input to help us understand filter flow and pressure drop characteristics.

### References

- (1) R.S. Brodkey, H.C. Hershey, *Transport Phenomena, A Unified Approach*, McGraw Hill, 1988.
- (2) A. H. Castillejos E., F.A. Acosta G., "Fluid-Dynamic Characterization of Ceramic Filters", CINVESTAV, Unidad, Saltillo, Mexico, (FOSECO Contracted Report), April 2000.
- (3) M.D.M. Innocentini, P. Sepulveda, V.R. Salvini, V.C. Pandolfelli, "Permeability and Structure of Cellular Ceramics: A Comparison Between Two Preparation Techniques", *American Ceramic Society Journal*, Vol 81, No. 12, pp. 3349-3352, 1998.
- (4) M.D.M. Innocentini, V.R. Salvini, A. Macedo, V.C. Pandolfelli, "Prediction of Ceramic Foams Permeability Using Ergun's Equation", *Materials Research*, Vol 2, No. 4, pp. 283-289, 1999.
- (5) M.D.M. Innocentini, V.R. Salvini, V.C. Pandolfelli, J.R. Coury, "Assessment of Forchheimer's Equation to Predict the Permeability of Ceramic Foams", *American Ceramic Society Journal*, Vol 82, No. 7, pp. 1945-1948, 1999.
- (6) M.D.M. Innocentini, V.R. Salvini, V.C. Pandolfelli, J.R. Coury, "The Permeability of Ceramic Foams", *The American Ceramic Society Bulletin*, September 1999.
- (7) M.D.M. Innocentini, A.R.F. Pardo, V.R. Salvini, V.C. Pandolfelli, "How Accurate is Darcy's Law for Refractories", *The American Ceramic Society Bulletin*, November 1999.
- (8) F.A. Acosta G., A.H. Castillejos E., J.M. Almanza R., A. Flores V., "Analysis of Liquid Flow Through Ceramic Porous Media Used for Molten Metal Filtration", *Metallurgical and Materials Transactions B*, Vol 26B, pp. 159-171, February 1995.
- (9) F.A. Acosta G., A.H. Castillejos E., "A Mathematical Model to Study Filtration Efficiency of Ceramic Foam Filters", *The Minerals, Metals and Materials Society, Fluid Flow Phenomena in Metals Processing*, pp. 229-236, 1999.
- (10) Lo, H. S. H., and Campbell, J., "The Modelling of Ceramic Foam Filters", *Modeling of Casting, Welding and Advanced Solidification Processes – IX*, August 2000.
- (11) E. Flender, "MAGMASOFT Version 4.0 Software and User's Manual", Jan 2000.
- (12) J. P. Day, "Pressure Drop in Cellular RTO/RCO Heat Exchange Media", 98-WA47B.03 (A704), 1998.